Generation of 40-as few-cycle pulse through chirp manipulation

Masoud Mohebbi and Saeed Batebi*

Department of Physics, Faculty of Science, University of Guilan No. 41335-19141, Rasht, Iran

**Corresponding author: s_batebi@guilan.ac.ir*

Received December 5, 2011; accepted February 25, 2012; posted online May 16, 2012

We discuss theoretically how supercontinuum spectra produced from high-order harmonic generation processes in a synthesized same-color laser field is optimized by adjusting the chirp parameter of the controlling pulse. Furthermore, a 40-attosecond isolated pulse with an effective bandwidth of 121 orders is obtained from He+ ion when the chirp rate ratio of pulses has a small value. The numerical results show that the efficiency of single as pulse generation is enhanced, and the quantum paths are controlled successfully. Our simulation shows that the produced pulses with high signal-to-noise ratio are obtained straightforwardly without any phase compensation. These results are explained using the classical approach.

OCIS codes: 190.0190, 140.0140.

doi: 10.3788/COL201210.081901.

High-order harmonic generation (HHG) has been of great interest due to its potential application as a coherent soft-X-ray source[1] and in the generation of attosecond (as) pulses[2,3]. Thus far, the HHG is considered the most promising approach in generating attosecond pulses. For practical application, the straightforward attosecond metrology prefers an isolated attosecond pulse, and as such, much effort has been exerted to obtain an isolated as pulse[4,5]. In the single-atom level, two of the most important methods of generating an isolated attosecond pulse involve the use of a few-cycle laser[6] and the polarization gating technique[7]. Control of quantum paths is another effective way of producing an isolated broadband ultrashort attosecond pulse[8]. To obtain a regular and intense short attosecond pulse, some promising ways have been proposed to control quantum paths, such as the two-color schemes[9,10] and preparing ions in a coherent superposition of the states[11]. Recently, Xu *et al.*[12] proved a combined same-color field scheme that can broaden the high-order harmonics plateau; they obtained an isolated 59-as pulse. In this letter, based on Ref. [12], we propose a method, in which the chirp of the laser pulse is controlled to generate a short and intense isolated broadband attosecond pulse. When the ratio of the chirp factors of the fundamental and controlling laser fields has a small value, the bandwidth of the harmonic plateau is broadened to 200 eV with some very slight modulations. Practically, to generate the 10 fs at 800-nm pulse, hollow fiber compression technique can easily be used[13]. For achieving more precise and accurate results and specially isolated attosecond with regular structure (i.e., without any phase compensation), we investigate the generation of high-order harmonics based on one-dimensional (1D) HHG calculations. We also used atomic units in all equations below.

To verify our scheme, we investigated the HHG and the attosecond pulse generation by solving numerically the 1D time-dependent Schrodinger equation for He^+ ion. We chose the soft-core Coulomb potential $V = -a/\sqrt{b+x^2}$ for He^+. We also set soft-core parameters to be $a = 2$ and $b = 0.5$, which can reproduce the ground-state binding energy of 2.0 a.u. for He^+. After the time-dependent wave function was determined, we then calculated the time-dependent induced dipole acceleration. The HHG power is proportional to the modulus-squared of the Fourier transform of induced dipole acceleration. The electric field of the synthesized laser pulse is expressed as

$$E(t) = E_0 \exp\left[-4\ln(2)\frac{t^2}{\tau^2}\right]\{\cos[\omega_0 t + \phi_1(t)] + \cos[\omega_0 t + \phi_2(t)]\}, \quad (1)$$

where E_0 is the amplitude, and ω_0 represents the frequencies of the driving and controlling fields, respectively. Moreover, τ is fixed at 9 fs, which corresponds to the pulse durations full-width at half-maximum (FWHM) of the two laser fields. $\phi_i(t) = -\beta_i \tanh(t/\tau_0)$ are the time profiles of the carrier envelope phase ($i = 1, 2$), and β_i and $\tau_0 = 200$ are employed to control the chirp forms.

We first calculated the single-atom spectrum from He^+ ion for the case where the chirp parameters for the synthesized laser field are ($\beta_1 = 6.25$, $\beta_2 = 0$), i.e., the same chirp condition considered in Ref. [12]. The 2 pulses are equally intense and their peak intensities are chosen as 5×10^{14} W/cm^2. As shown by the black solid curve in Fig. 1, the harmonic spectrum of this synthesized driving field exhibits a low modulated plateau. Clearly, the harmonics are almost continuous and smooth from the 412th to 480th order (i.e., 105 eV), providing the potential probability generating an isolated attosecond pulse. Next, we consider HHG from the synthesized laser pulses for $\beta_2 =$ 1.25 and 2.25, respectively, with fixed β_1 in 6.25. For the $\beta_2 = 1.25$ case, the cutoff position of the harmonic spectrum is significantly extended to the 540th order harmonic, as shown by the blue dotted curve in Fig. 1.

The harmonic spectrum also shows a structure with two plateaus. The width of the second plateau in the β_2 = 1.25 case is extended from the 257th to 545th order.

The efficiency of the second plateau for the $\beta_2 = 1.25$ case is higher than that of the $\beta_2 = 0$ case. The modulation of the second plateau for the $\beta_2 = 1.25$ case is smaller than that of the $\beta_2 = 0$ case. The harmonics from the 430th to 545th order is much smoother without

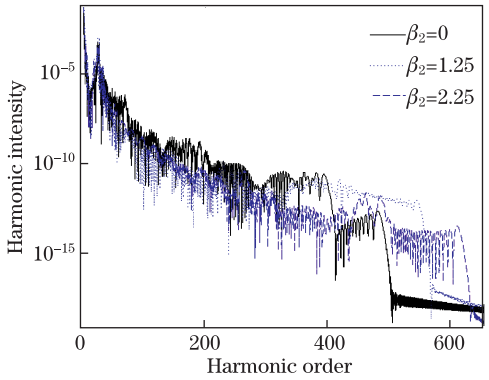

Fig. 1. (Color online) HHG power spectra of a He^+ ion in a synthesized laser field for the β_2 =0 case (black solid curve), the β_2 =1.25 case (blue dotted curve), and the β_2 =2.25 case (magenta dashed curve). The synthesized laser field is a β_1-6.25, 9-fs 800-nm pulse and a β_2-0, 9-fs 800-nm pulse. The intensity of the pulses is 5×10^{14} W/cm^2.

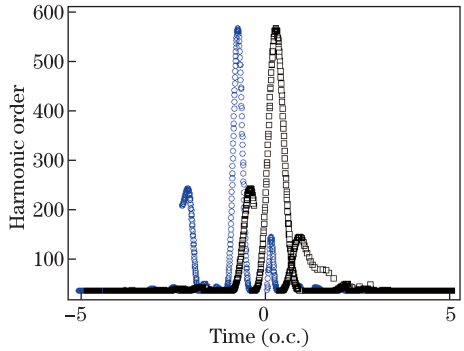

Fig. 2. (Color online) Dependence of harmonic order on the ionization time (blue circles) and the emission time (black square) in the synthesized laser field by a β_1-6.25, 9-fs 800-nm pulse and a β_2-1.25, 9-fs 800-nm pulse. The intensity of the pulses is 5×10^{14} W/cm^2.

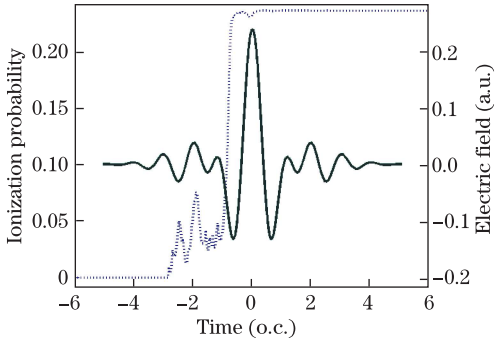

Fig. 3. (Color online) A synthesized laser pulse (green solid curve) and the time dependence of the ionization probability is irradiated by this field (blue dotted curve). The driving field parameters are the same as those in Fig. 2.

large modulation (ultrabroad extreme ultraviolet XUV supercontinuum), and is about 3 orders of magnitude higher than the case without chirp ($\beta_2 = 0$).

Thus, it is possible to use the high-efficiency continuous spectrum to obtain an intense isolated short as pulse. When the β_2 factor increases to 2.25, as shown by the magenta dashed curve in Fig. 1, the second cutoff position is extended to the 610th order harmonic. Furthermore, the second plateau composed of 110 orders (from 500th to 610th) is broader than that for the β_2 = 0 case, and the modulation of the second plateau is enhanced. The other chirp parameters do not indicate significant results. Thus, the β_2 = 1.25 case is the optimum chirp parameter of controlling field for generating intense isolated as pulses. This can be explained easily by the classical model of HHG[14] and the ionization probability. Figure 2 presents the dependence of the kinetic energies (harmonics order) on the ionization (blue circles) and recombination times (black square) for the driving laser field that synthesized the field by a β_1-6.25, 800-nm chirped pulse and a β_2-1.25, 800-nm chirped pulse (green solid curve in Fig. 3). The harmonics from the 250th to 566th order are associated with the electrons ionized between –0.90 and –0.58 optical cycles (o.c) (Fig. 2). In this range of harmonics, there are two dominant quantum paths that form the second plateau. Electrons with the long paths are ionized mainly from –0.90 to –0.74 o.c, and electrons with the short paths are ionized mainly from –0.74 to –0.58 o.c. The blue dotted curve in Fig. 3 exhibits the ionization as a function of time. In this region, the ionization probability between –1.08 and –0.74 o.c is much higher than those at other moments (Fig. 2). In addition, electrons with long paths travel a longer time in the continuous state, resulting in a lower harmonic efficiency due to quantum diffusion [11]. Therefore, the harmonic efficiencies of the long paths are much higher than those for the short paths, which can be found from the blue dotted curve in Fig. 1. This indicates that the long quantum path control can be achieved using the 800-nm chirp-free laser pulse.

For the harmonics below the 250th order, the interference between multi quantum paths leads to irregular spectrum structure (Fig. 2). An isolated attosecond pulse can be obtained when only a single quantum path contributes to the HHG.

The temporal profile can be obtained by superposing several orders of the harmonics. Figure 4 shows the attosecond pulses generated from He^+ ions. By superposing the harmonics ranging from the 415th to 475th order in the synthesized laser pulse for the $\beta_2 = 0$ case, a regular 61-as burst and a weak burst are observed in one cycle (Fig. 3, black solid curve). For the $\beta_2 = 1.25$ case, by

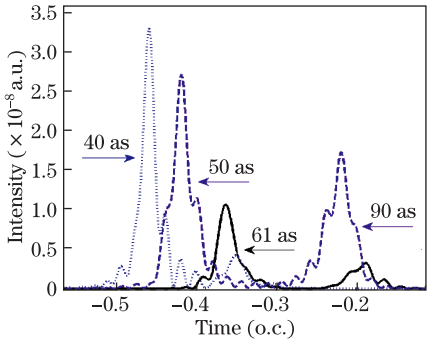

Fig. 4. (Color online) Temporal profiles of by superposing the harmonics from the 415th to 475th order (blue solid curve), the 400th to 465th order (magenta dashed curve) and the 540th to 600th order (magenta dashed curve). The black solid and magenta dotted curves have been multiplied by factors of 40 and 250, respectively, for the purpose of comparison and clarity.

selecting harmonics from the 400th to 465th order (blue dotted curve), one can see clearly that an intense isolated 40-as pulse with several small satellites is obtained straightforwardly without any phase compensation (Fig. 3). The intensity ratio of the large satellite pulse to the main pulse is below 9%. Finally, for the $\beta_2 = 2.25$ case, the magenta dashed curve shows that 2-as bursts are generated by superposing harmonics from the 540th to 600th order (Fig. 4). The strong as burst and the weak one are 50 and 90 as, respectively. The intensity of the prepulse is higher than that of the postpulse, and the intensities of the 2-as pulses are lower than the $\beta_2 = 1.25$ case. These indicate that both the intensity and the time profile of the attosecond pulses have a certain degree of dependence on the relative chirping parameters.

In conclusion, We investigate theoretically the HHG and attosecond pulse in a He^+-like model ion. We use the combined laser pulses composed of a moderate-intense 800-nm chirped pulse and a controlling one. Here, the multicycle 800-nm pulse is adopted, through which we demonstrated that the introduction of chirping to a controlling laser field is an efficient way to extend the broadband continuum spectrum and the frequency cut off order. Moreover, by adding a chirp to the controlling pulse, the quantum paths in HHG can be controlled effectively and the efficiency of the second plateau can be enhanced by three orders of magnitude in comparison with chirp-free case. In moderate intensity of multicycle pulses, by adjusting the frequency sweeping range ratio to small and non-zero values, an XUV supercontinuum with the bandwidth of 315 orders can be observed. By superposing a proper range of harmonics in the supercontinuum, an efficient 40-as isolated pulse can be obtained straightforwardly. As a result, clean harmonic spectra and strong and regular as pulse with high signal-to-noise ratio are obtained without any phase compensation. To explain these results the electronic dynamic of the HHG has been analyzed using the semiclassical model.

References

1. M. Drescher, M. Hentschel, R. Kienberger, G. Tempea, C. Spielmann, G. A. Reider, P. B. Corkum, and F. Krausz, Science **291,** 1923 (2001).
2. E. Goulielmakis, M. Schultze, M. Hofstetter, V. S. Yakovlev, J. Gagnon, M. Uiberacker, A. L. Aquila, E. M. Gullikson, D. T. Attwood, R. Kienberger, F. Krausz, and U. Kleineberg, Science **320,** 1614 (2008).
3. R. Kienberger, E. Goulielmakis, M. Uiberacker, A. Baltuska, V. Yakovlev, F. Bammer, A. Scrinzi, T. Westerwalbesloh, U. Kleineberg, U. Heinzmann, M. Drescher, and F. Krausz, Nature **42,** 81 (2004).
4. M. Hentschel, R. Kienberger, C. Spielmann, G. A. Reider, N. Milosevic, T. Brabec, P. Corkum, U. Heinzmann, M. Drescher, and F. Krausz, Nature **414,** 509 (2001).
5. J. Wu, G. Zhang, C. Xia, and X. Liu, Phys. Rev. A **82,** 013411 (2010).
6. P. Lan, E. J. Takahashi, and K. Midorikawa, Phys. Rev. A **82,** 053413 (2010).
7. M. Ivanov, P. B. Corkum, T. Zuo, and A. Bandrauk, Phys. Rev. Lett. **74,** 2933 (1995).
8. S. Zhao, X. Zhou, P. Li, and Z. Chen, Phys. Rev. A **78,** 063404 (2008).
9. C. M. Kim and C. H. Nam, J. Phys. B **39,** 3199 (2006).
10. W. Hong, P. W. Cao, P. Lan, and X. Wang, J. Phys. B **40,** 2321 (2007).
11. J. Chen, Y. Yang, S. Zeng, and H. Liang, Phys. Rev. A **83,** 023401 (2011).
12. J. Xu, B. Zeng, and Y. Yu, Phys. Rev. A **82,** 053822 (2010).
13. M. Nisoli, S. D. Silvestri, and O. Svelto, Appl. Phys. Lett. **68,** 2793 (1996).
14. P. B. Corkum, Phys. Rev. Lett. **71,** 1994 (1993).